Supplementary materials

Synergistic Band Gap Expansion and Grain Refinement toward High Thermoelectric Efficiency and Robust Mechanics in p-Type $(Bi, Sb)_2Te_3$

Jie Zheng[a], Ruiheng Li[a], Zhilong Zhao[a], Fan Feng[a], Xiang An[a], Shengqiang Cui[a], Longqing Chen[a,*], Ran Ang[a,b,c,*]

[a] *Key Laboratory of Radiation Physics and Technology, Ministry of Education, Institute of Nuclear Science and Technology, Sichuan University, Chengdu, Sichuan 610064, China*

[b] *College of Physics, Sichuan University, Chengdu 610064, China*

[c] *Institute of New Energy and Low-Carbon Technology, Sichuan University, Chengdu 610065, China*

*E-mails: rang@scu.edu.cn; chenlongqing@scu.edu.cn

Supplementary Methods

1. Method of Synthesis

The Ag_9GaSe_6 polycrystalline samples were prepared via direct reaction with Ag (99.999%), Ga (99.99%), and Se (99.999%) by accurately weighed. Subsequently, the raw materials were sealed in silica tubes under vacuum at 10^{-3} Torr. The ingots were kept at 1373 K for 12 hours and then quenched in cold water. Finally, the quenched ingots were annealed at 873 K for 5 days.

Polycrystalline $Bi_{0.3}Sb_{1.7}Te_3$ (BST) was synthesized using high-purity elements: Bi (99.99%), Sb (99.999%), and Te (99.999%). The mixture was loaded into Ø20 mm quartz tube and flame sealed at a residual pressure of 10^{-3} Torr. It was heated to 1073 K within 5 h, held at this temperature for 6 h, and then cooled to room temperature over 10 h within the furnace.

The previously synthesized BST and Ag_9GaSe_6 were weighed and combined according to the stoichiometric proportion of BST + x wt.% Ag_9GaSe_6 (x = 0, 0.05, 0.15, 0.25, 0.35). They were manually ground into small pieces using an agate mortar and pestle. These pieces were placed into an 80 ml ball mill jar filled with Ar and ball milled (MSK-SFM-3-I) at a vibration frequency of 1800 r/min for 30 min. Finally, the powder was poured into a Ø12.7 mm graphite mold and compacted by hot press at 693 K, 50 MPa for 15 min under a vacuum ($<$5 Pa).

2. Structural and mechanical properties characterization

Room-temperature X-ray diffraction (XRD) analyses were carried out using an X-ray

diffractometer equipped with Cu Kα (λ = 1.5406 Å) radiation. The XRD spectra of all samples were subjected to Rietveld structure refinement. The microstructures and elemental compositions of the samples were examined by a field emission scanning electron microscope (SEM, FEI Inspect F50) equipped with the energy-dispersive spectrometer (EDS). Additionally, the microhardness was measured 10 times using a Vickers diamond indenter on the HVS-1000 system on the load of 2 N for 10 s at room-temperature.

3. Thermoelectric property measurements

The electrical conductivity (σ) and Seebeck coefficient (S) from 300 to 500 K were measured in a vacuum via a CTA pro instrument of Beijing Cryoall Science and Technology Co., Ltd (China), and the bulks were cut and polished into bars with sizes of 9 mm × 2.5 mm × 2.5 mm for testing. The thermal conductivity (κ) was obtained by the equation: $\kappa = \rho \times D \times C_p$, where ρ is geometrical density and obtained by Archimedes method, C_p is the heat capacity obtained via the Dulong Petit limit, and D is the thermal diffusivity gauged by the laser flash technique(LFA 467, Netzsch) under argon flow, and samples with ≈ 1.1 mm in thickness and 12.5 mm in diameter. The Hall coefficient (R_H) was tested by the Van der Pauw method under a reversible magnetic field of 1.5 T at room temperature, and the carrier concentration (p_H) and carrier mobility (μ_H) were calculated via the expression: $p_H = 1 / (e \times R_H)$ and $\mu_H = \sigma \times R_H$, respectively, where e is the elementary charge. Owing to the anisotropic nature of bismuth telluride, the electrical and thermal properties were measured parallel to the uniaxial HP pressure (out-of-plane direction), as detailed in **Fig. S4**.

4. TE module

The TE modules included 7 pairs of p-n legs with an overall size of 1.4 mm × 1.4 mm × 3 mm, where p-type legs were preparative of $Bi_{0.3}Sb_{1.7}Te_3$ + 0.15 wt.% Ag_9GaSe_6, and the composition of n-

type legs used hot extrusion $Bi_2Te_{2.7}Se_{0.3}$. For details TE properties of n-type legs, please refer to **Fig. S6**. Nickel layers were electroplated as the diffusion barrier layer on the upper and lower surfaces of the TE legs. These 7-pair TE legs were bonded directly in series onto a copper direct-bonded ceramic (DBC) substrate with $Sn_{90}Sb_{10}$ solder (melting point ~260 °C). The output performance of TE modules was measured using a home-built test system. The relevant experimental setup and principles detailed have been reported in previous literature[1, 2].

5. The effective mass modeling

Through the single parabolic band (SPB) and considering acoustic phonon scattering. The Seebeck coefficient can be expressed as:[3]

$$S = \frac{k_B}{e}\left[\frac{(r+5/2)F_{r+3/2}(\eta)}{(r+3/2)F_{r+1/2}(\eta)} - \eta\right] \tag{S1}$$

where η is the reduced Fermi energy, k_B is the Boltzmann constant, e is the electron charge, and r = -1/2 is the scattering factor when the charge carriers are mainly scattered by acoustic phonons.

$$F_j = \int_0^\infty \frac{x^j\,dx}{1+e^{(x-\eta)}} \tag{S2}$$

The carrier concentration n_H:

$$n_H = \frac{16\pi\left(2m^* k_B T\right)^{1.5}}{3h^3}\frac{F_0^2}{F_{-0.5}} \tag{S3}$$

where m^* is the density of state (DOS) effective mass, h is the Plank's constant, T is the absolute temperature. The mobility μ_H:

$$\mu_H = \mu_0 \frac{F_{-1/2}}{2F_0} = \frac{\tau_0 e F_{-1/2}}{m^* \cdot 2F_0} \tag{S4}$$

where τ_0 is relaxation time, and can be expressed as:

$$\tau_0 = \frac{h^4 C_l}{8\sqrt{2}\pi^3 E_{\mathrm{def}}^2 m^* kT^{3/2}} \tag{S5}$$

where C_l is a parameter determined by the combination of the elastic constant, E_{def} is a combination of deformation potentials for multivalley systems[4, 5].

Hall factor A is given by:

$$A = \frac{3}{2} F_{1/2}(n) \frac{F_{-1/2}}{2F_0^2} \tag{S6}$$

The Lorentz factor (L) is given by

$$L = \frac{k_{\mathrm{B}}^2 \left(3F_0F_2 - 4F_1^2\right)}{e^2 \cdot F_0^2} \tag{S7}$$

6. The calculation of bipolar thermal conductivity (κ_{b})[6]

To calculate the electron carrier concentration (n_{e}) at 300 K is applied as follows:

$$n_{\mathrm{e}} = 4\pi \left(\frac{2m_{\mathrm{e}}^* k_{\mathrm{B}} T}{h^2} \right)^{3/2} F_{1/2}(\eta_{\mathrm{e}}) \tag{S8}$$

where h is the Planck constant, m_{e}^* is the effective mass of the electrons.

$$(n_{300\,\mathrm{K}} + \Delta)(p_{300\,\mathrm{K}} + \Delta) = AT^3 \exp\left(-\frac{E_{\mathrm{g}}}{k_{\mathrm{B}} T} \right) \tag{S9}$$

Δ denotes the excitation concentration of electron-hole pairs at temperature T. The values of constant A are presented in **Table S1**.

In n-type Bi_2Te_3-based materials, phonon scattering is the predominant carrier scattering mechanism at 300 K. Therefore, the electron mobility (μ_{e}) also follows the relation $\mu_{\mathrm{e}} \sim T^{-3/2}$.

According to **Fig. S3b**, we find that the calculated electron concentration (n) for all samples follows the same empirical relation $n \sim T^7$. Thus, the qualitative expression between μ_e and n are derived $\mu_e \approx Bn^{-1/5}$, where B is a temperature-independent constant at a fixed composition. Then the electron partial electrical conductivity σ_e is calculated based on parameter B and electron concentrations.

In the next numerical modeling process, B is set as an adjustable parameter and listed in **Table S1**. Then, **Equation 5** is approximately changed to

$$\kappa_b = \left(\frac{k_B}{e}\right)^2 T\left(4+\frac{E_g}{k_B T}\right)^2 \cdot \frac{Bn^{\frac{4}{5}} \cdot p\mu_H}{Bn^{\frac{4}{5}} + p\mu_H} \tag{S10}$$

where e is the free electron charge, μ_H is the hole mobility, and p_H is the hole concentration. The μ_H above 300 K can be extrapolated by using the measured low temperature Hall data according to the relationship of $\mu_H\ (T) \sim T^{-3/2}$. The p_H values above 300 K were calculated using **Equation S9**. Then, the temperature dependence of κ_b is shown in **Fig. 5d**.

7. The calculation of lattice thermal conductivity (κ_l)

Based on the Debye-Callaway model[7], the spectral lattice thermal conductivity (κ_s) after doping or alloying can be estimated by the following equation:

$$k_s(\omega) = \frac{k_B}{2\pi^2 v}\left(\frac{k_B T}{\mathrm{h}}\right)^3 \tau_{tot}(x)\frac{x^4 e^x}{(e^x-1)^2} \tag{S11}$$

$$v = \left[\frac{1}{3}\left(\frac{1}{v_L^3}+\frac{2}{v_T^3}\right)\right]^{-1/3} \tag{S12}$$

where $x = \hbar\omega/k_B T$ (ω denoting the phonon frequency) is the reduced phonon frequency, $\hbar$ is the reduced Plank constant, k_B is the Boltzmann constant, v is average sound speed, the v_L and v_T denoting the

longitudinal and transverse sound velocities, respectively. τ_{tot} is the total relaxation time and can be evaluated via the Matthiessen's rule.

$$\tau_{tot}^{-1} = \tau_{UN}^{-1} + \tau_{PD}^{-1} + \tau_{GB}^{-1} \tag{S13}$$

Here, we mainly consider phonon-phonon Umklapp scattering (UN), grain boundary scattering (GB), and point defect scattering (PD).

The Umklapp phonon-phonon scattering (UN):

$$\tau_{UN}^{-1} = A_N \frac{2}{(6\pi^2)^{\frac{1}{3}}} \frac{k_B V^{\frac{1}{3}} \gamma^2 \omega^2 T}{M v^3} \tag{S14}$$

where A_N is the prefactor of Umklapp scattering time, V is the average atomic volume, γ is the Grüneisen parameter, M the average atomic mass.

The grain boundary phonon scattering (GB):

$$\tau_{GB}^{-1} = \frac{v}{d} \tag{S15}$$

where d is the average grain size.

The point defect phonon scattering (PD):

$$\tau_{PD}^{-1} = \frac{V\omega^4}{4\pi v^3} \Gamma \tag{S16}$$

where Γ is the point defect scattering parameter and determined as:

$$\Gamma = x(1-x)\left[\left(\frac{\Delta M}{M}\right)^2 + \frac{2}{9}\left\{(G+6.4\gamma)\frac{1+r}{1-r}\right\}^2 \left(\frac{\Delta a}{a}\right)^2\right] \tag{S17}$$

where x, ΔM, G, r, and Δa are the fractional concentration of either of constituents, the difference in mass, the parameter representing a ratio of fractional change of bulk modulus to that of local bond length, Poisson's ratio, and the difference in lattice constant, respectively. The parameters required for the Debye-Callaway model are summarized in **Table S2**.

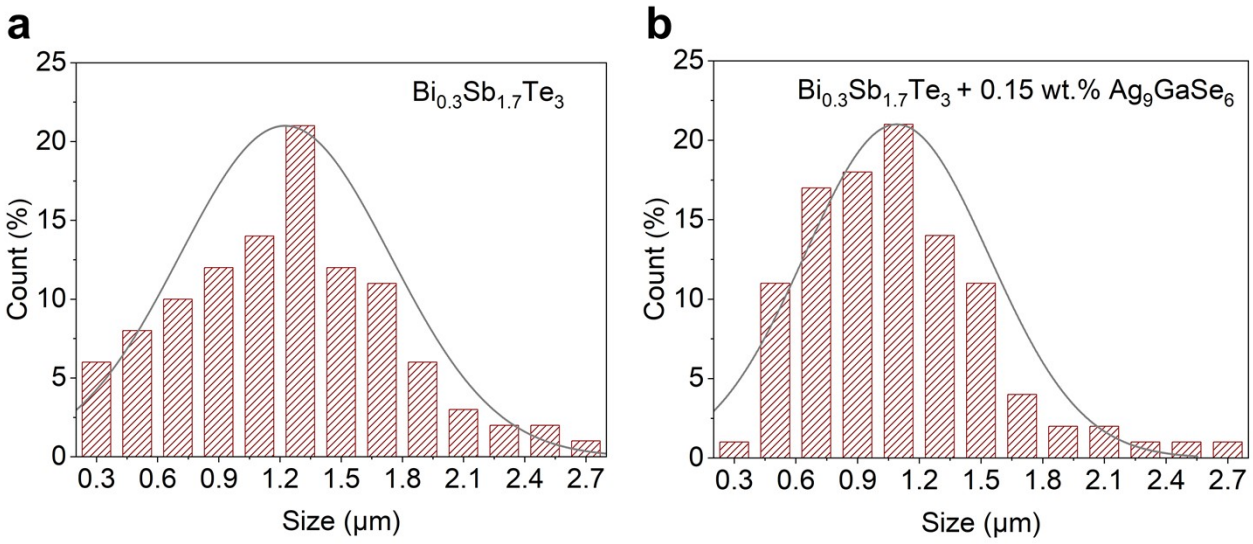

Fig. S1. Grain size distributions of fracture surfaces for (a) pristine $Bi_{0.3}Sb_{1.7}Te_3$ and (b) $Bi_{0.3}Sb_{1.7}Te_3$ + 0.15 wt.% Ag_9GaSe_6.

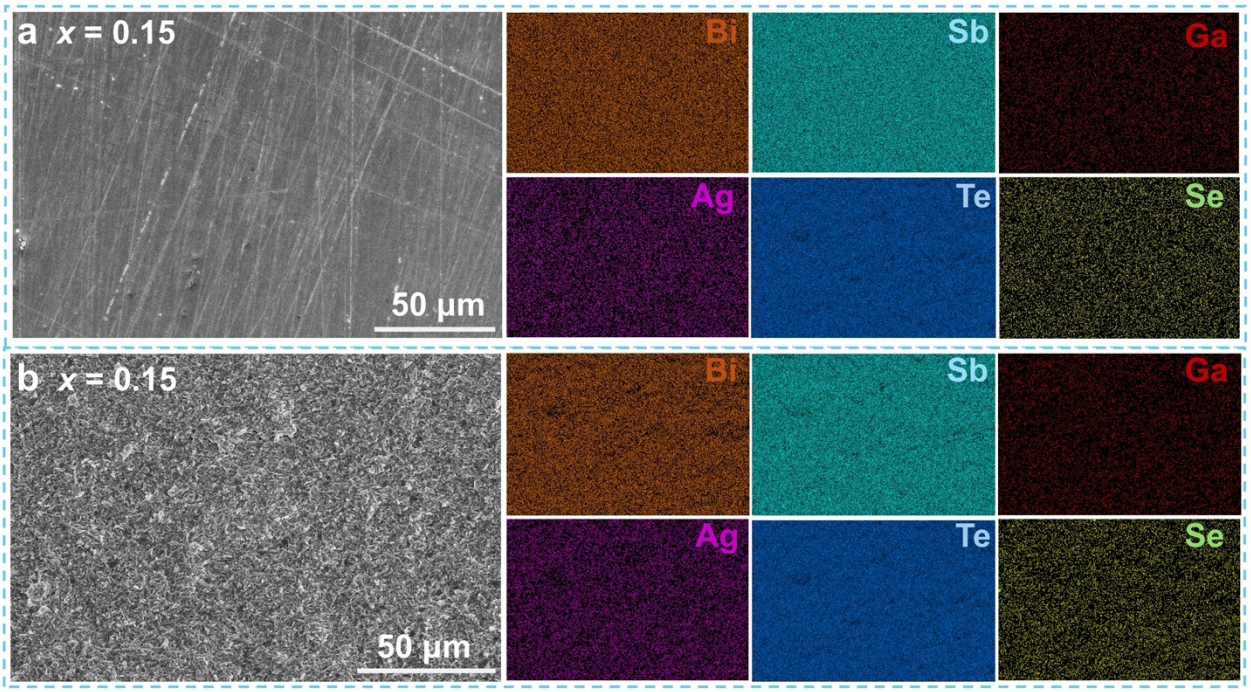

Fig. S2. Scanning electron microscope (SEM) images and corresponding energy dispersive spectroscopy (EDS) spectra of the polished and fractured surfaces of $Bi_{0.3}Sb_{1.7}Te_3$ + 0.15 wt.% Ag_9GaSe_6.

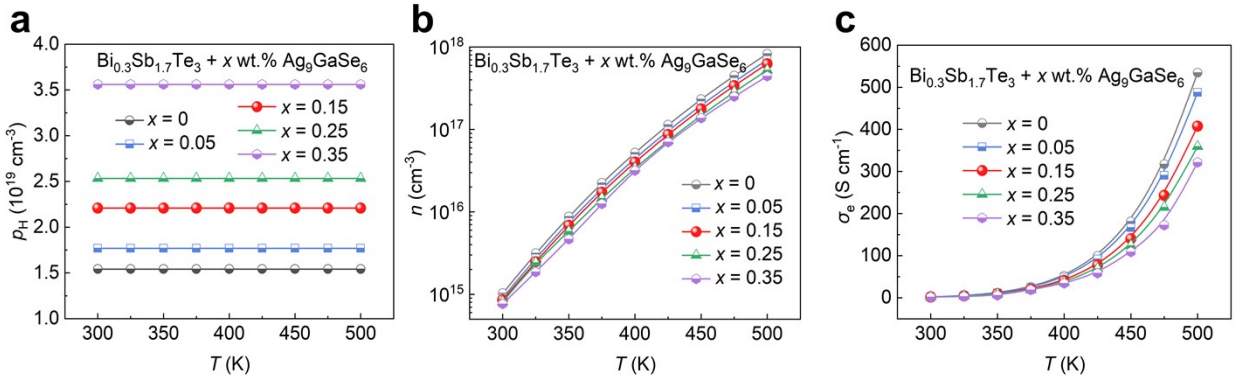

Fig. S3. Temperature-dependence of calculated electronic properties of $Bi_{0.3}Sb_{1.7}Te_3$ + x wt.% Ag_9GaSe_6 samples over 300-500 K: (a) hole concentration (p_H), (b) electron concentration (n), and (c) electrical conductivity (σ_e).

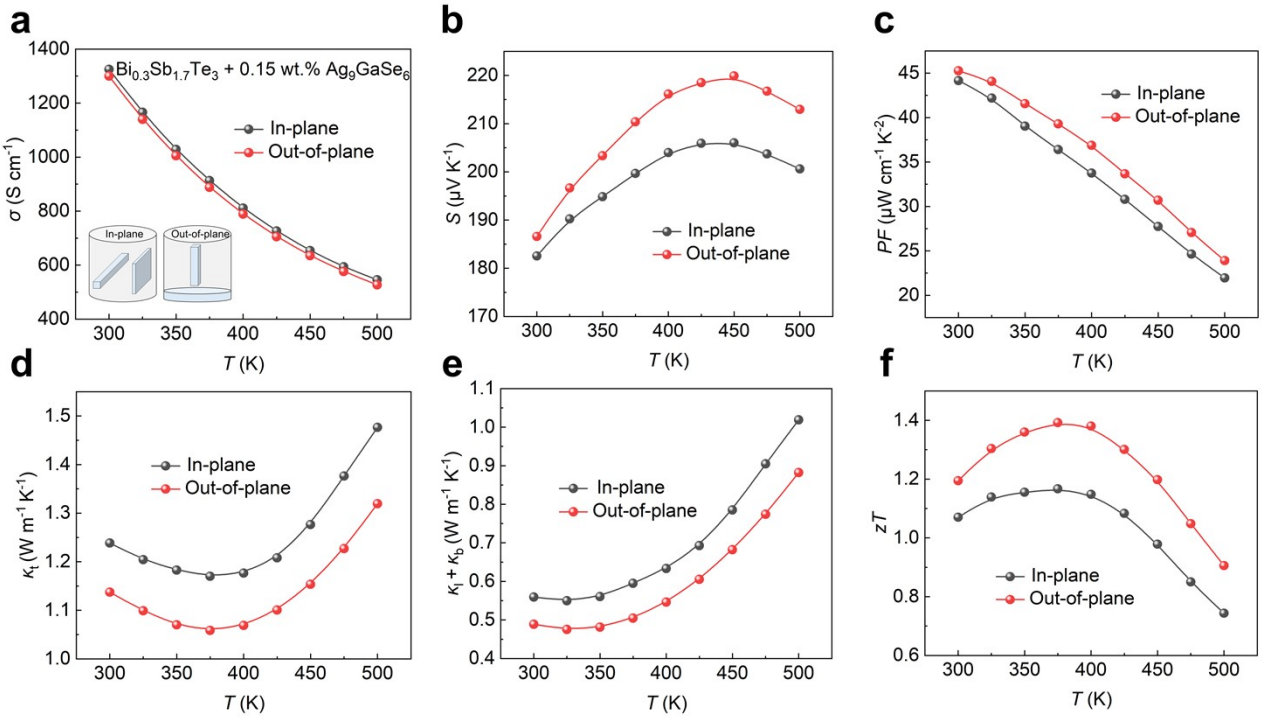

Fig. S4. Thermoelectric properties of $Bi_{0.3}Sb_{1.7}Te_3$ + 0.15 wt.% Ag_9GaSe_6 measured parallel (out-of-plane) and perpendicular (in plane) to the hot-pressing direction: (a) electrical conductivity (σ), (b) Seebeck coefficient (S), (c) power factor (PF), (d) total thermal conductivity (κ_t), (e) lattice plus bipolar thermal conductivity ($\kappa_l + \kappa_b$), and (f) figure of merit (zT).

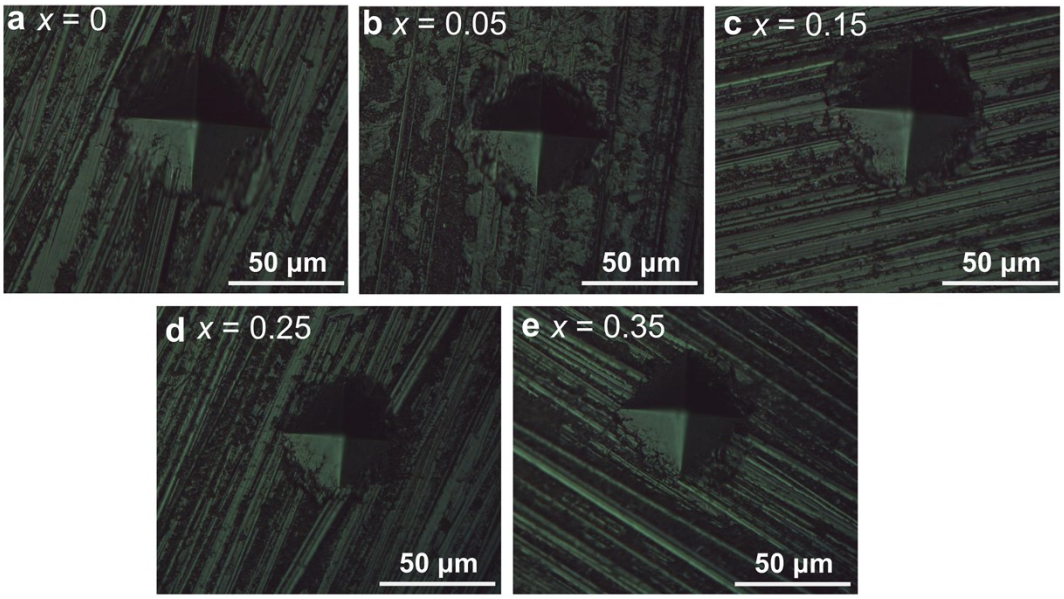

Fig. S5. Representative Vickers microhardness indentation images of $Bi_{0.3}Sb_{1.7}Te_3 + x$ wt.% Ag_9GaSe_6 samples.

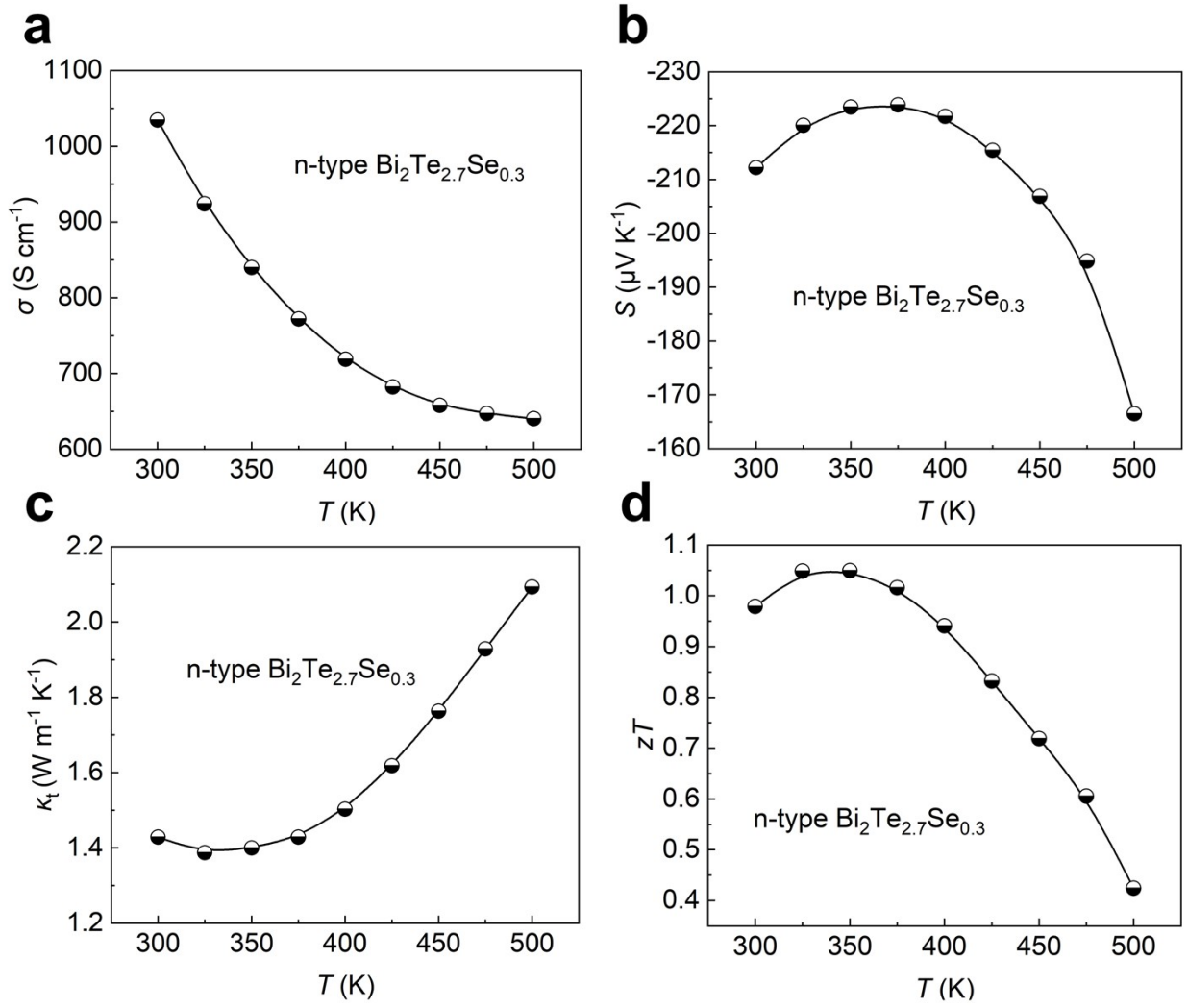

Fig. S6. Temperature-dependent thermoelectric properties of n-type $Bi_2Te_{2.7}Se_{0.3}$: (a) electrical conductivity, (b) Seebeck coefficient, (c) total thermal conductivity, and (d) *zT*.

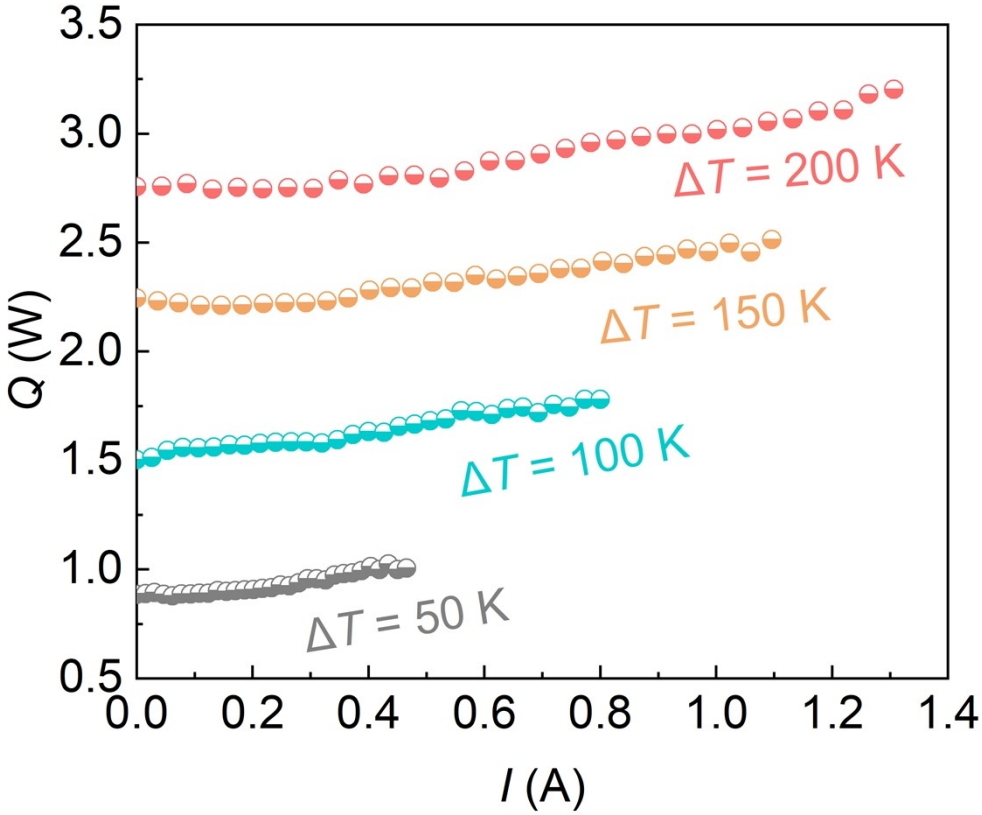

Fig. S7. Measured heat flow (Q) as a function of current (I) for the thermoelectric device at different temperature differences (ΔT).

Table S1. Calculated parameter A at 300 K using **Equation S9**. Parameter B was obtained by fitting the experimental bipolar thermal conductivity (κ_b) using **Equation S10**.

$Bi_{0.3}Sb_{1.7}Te_3 + x$ wt.% Ag_9GaSe_6	$x = 0$	$x = 0.05$	$x = 0.15$	$x = 0.25$	$x = 0.35$
A (10^{42} cm^{-6})	1.34	1.35	1.54	1.72	2.27
B (10^3)	1.15	1.33	1.29	1.42	2.63

Table S2. Parameters for the calculation of lattice thermal conductivity.

Parameters	Description	Values	Ref.
θ_D	Debye temperature	124	Ref.[8]
v	Average sound velocity	2147 m·s^{-1}	Ref.[9]
A_N	Comprehensive coefficient between Umklapp and Normal processes	2.26	fitted.
$\bar{V}$	Average atomic volume of $Bi_{0.3}Sb_{1.7}Te_3$	3.13×10^{-29} m^3	Ref.[9]
$\bar{M}$	Average atomic mass of $Bi_{0.3}Sb_{1.7}Te_3$	2.2×10^{-25} kg	fitted.
γ	Grüneisen parameter	2.3	Ref.[8]
r	Poisson's ratio	0.25	Ref.[8]
v_L	Longitudinal sound velocity	2988 m·s^{-1}	Ref.[8]
v_T	Transverse sound velocity	1721 m·s^{-1}	Ref.[8]
Γ	Point defect scattering parameter	0.175	Ref.[8]
d	Grain size	1.1×10^{-6} m	Exp.

References:

1. Q. Deng, X.-L. Shi, M. Li, X. Tan, R. Li, C. Wang, Y. Chen, H. Dong, R. Ang and Z.-G. Chen, *Nature Communications*, 2025, **16**, 656.
2. Q. Deng, F. Zhang, X. Yang, R. Li, C. Xia, P. Nan, Y. Chen, B. Ge, R. Ang and J. He, *Energy & Environmental Science*, 2024, **17**, 9467-9478.
3. J. Zhu, X. Zhang, M. Guo, J. Li, J. Hu, S. Cai, W. Cai, Y. Zhang and J. Sui, *npj Computational Materials*, 2021, **7**, 116.
4. Y. Xiao, H. Wu, W. Li, M. Yin, Y. Pei, Y. Zhang, L. Fu, Y. Chen, S. J. Pennycook, L. Huang, J. He and L.-D. Zhao, *Journal of the American Chemical Society*, 2017, **139**, 18732-18738.
5. H. Li, L. Chen, Z. Guo, G. Wu, X. Tan, Q. Zhang, J. Cai, Q. Sun, J. G. Noudem, P. Sun, J. Wu, G.-Q. Liu and J. Jiang, *Energy & Environmental Science*, 2024, **17**, 6091-6101.
6. F. Hao, P. Qiu, Y. Tang, S. Bai, T. Xing, H. S. Chu, Q. Zhang, P. Lu, T. Zhang, D. Ren, J. Chen, X. Shi and L. Chen, *Energy and Environmental Science*, 2016, **9**, 3120-3127.
7. J. Callaway and H. C. von Baeyer, *Physical Review*, 1960, **120**, 1149-1154.
8. H. L. Zhuang, H. H. Hu, J. Pei, B. Su, J. W. Li, Y. L. Jiang, Z. R. Han and J. F. Li, *Energy and Environmental Science*, 2022, **15**, 2039-2048.
9. Q. Zhang, M. Yuan, K. Pang, Y. Zhang, R. Wang, X. Tan, G. Wu, H. Hu, J. Wu, P. Sun, G. Q. Liu and J. Jiang, *Advanced Materials*, 2023, **35**, 2300338.